

Covid-19 vaccination strategies with limited resources—a model based on social network graphs

Simone Santini

Universidad Autónoma de Madrid

Abstract

We develop a model of infection spread that takes into account the existence of a vulnerable group as well as the variability of the social relations of individuals. We develop a compartmentalized power-law model, with power-law connections between the vulnerable and the general population, considering these connections as well as the connections among the vulnerable as parameters that we vary in our tests.

We use the model to study a number of vaccination strategies under two hypotheses: first, we assume a limited availability of vaccine but an infinite vaccination capacity, so that all the available doses can be administered in a short time (negligible with respect to the evolution of the epidemic). Then we assume a limited vaccination capacity, so that the doses are administered in a time non-negligible with respect to the evolution of the epidemic.

We develop optimal strategies for the various social parameters, where a strategy consists of (1) the fraction of vaccine that is administered to the vulnerable population and (2) the criterion that is used to administer it to the general population. In the case of a limited vaccination capacity, the fraction (1) is a function of time, and we study how to optimize it to obtain a maximal reduction in the number of victims.

1 Introduction

A number of projects for the development of a vaccine for the SARS-cov2 virus are in advanced stages of development and clinical trials [24, 8, 19, 13, 16, 2, 11], and it seems possible that by the first or second trimester of 2021, a tested, off-the-lab vaccine could be available. However, off-the-lab availability is not enough: the vaccine will have to be produced and distributed in great quantities, and this will take time. The dire reality of world power makes it quite likely that the early production will be distributed mainly in the richest and most powerful countries, while many countries will initially receive an amount insufficient to vaccinate more than a fraction of the population. This state of affairs poses the problem of designing a vaccination strategy: who should be vaccinated first so that the limited amount of vaccine will have a maximum impact, at least while the country is waiting for more substantial amounts to be delivered? A general consensus is that medical and paramedical personnel, crucial in an epidemic, should be the first to receive the vaccine. However, assuming that once the essential personnel has been vaccinated there are still doses available, one faces the problem of how to distribute this surplus among the general

population to minimize the number of casualties while the country waits for more vaccine to arrive.

We develop here an infection spread model suitable for studying vaccination strategies in the presence of a vulnerable portion of the population, and we use it to begin a study of vaccination schedules under various hypotheses regarding the constraints that the limited availability of vaccine or the limited vaccination capacity may impose.

The most common models in the study of epidemic diffusion are derivations of the standard SIR model [10, 1, 25, 23], which makes strong hypotheses about the distribution of the population and its interactions. In all these models, if $S(t)$ and $I(t)$ are the numbers of susceptible (healthy) and infected people at time t , the probability that a healthy person enters in contact with an infected one is proportional to $S(t)I(t)$. Because of this, the model doesn't account for the different sizes of social circles that different people may have [6, 7, 9], thereby not allowing the modeling of targeted vaccination strategies.

We define a richer model of social interaction, one that takes into account the variability of social circles, and use it to simulate and evaluate various vaccination strategies. We consider a general model and ground it using the social and epidemiological data from Spain as a test-bed¹.

The model divides the population in two groups: a more vulnerable group (conventionally referred to here as the *elderly*) and a less vulnerable one (the *young*). The parameters for the two groups have been set considering the Spanish population age 20–64 for the young, and age ≥ 65 for the elderly. The social connections among the young have been estimated using average social circle data [26]. The social connections within the group of elderly, as well as between elderly and young, are parameters that we vary in our tests.

Using this model, we test various scenarios that differ in the fraction of vaccine that is administered to the elderly as well as in the policy that we use to decide which young should be vaccinated first. We also consider the case in which the vaccination capacity is limited and the vaccine must be administered over an extended period of time, not negligible with respect to the spread of the epidemic. In this case, we use a genetic optimization algorithm to design an optimal vaccination schedule.

2 The Model

Social groups are customarily modeled as random graphs in which nodes represent individuals and edges represent social interactions between individuals [6, 20, 21]. Let $G = (V, E)$ be such a graph, with $V = \{1, \dots, N\}$ and $E \subseteq V \times V$. We assume that the graph is undirected without self-loops ($(u, v) \in E \Leftrightarrow (v, u) \in E$ and $(u, u) \notin E$ for all u, v), and let $m = |E|/2$ be the number of edges². The *neighbor* of a node is

$$N(u) = \{v \mid (u, v) \in E\} \tag{1}$$

¹The epidemiological data are derived from the daily reports from the *Ministerio de Sanidad*, published in the web page www.mscbs.gob.es/en/profesionales/saludPublica/ccayes/alertasActual/nCov/home.htm

²The factor 2 is due to the fact that each arc between u and v is represented twice in E , once as (u, v) and once as (v, u) .

and its *degree* is $d(u) = |N(u)|$. We indicate with $\bar{d} = \sum_k d(k)/N$ the average number of neighbors of nodes in the graph. Let $P_k = \mathbb{P}_u[d(u) = k]$ the probability that a random node, selected with uniform probability, had degree k . One crucial observation in most social networks is the existence of relatively few people with many contacts, and a "long tail" of many people with less and less social contacts [5, 27, 14, 22]. Specifically, many a social network exhibit a *power law* or *scale-free* distribution of the type $P_k \sim k^{-\gamma}$ where $\gamma > 1$ is an exponent that determines how "fat" the log tail is, and that depends on the specific social network [18, 4].

Several random graph models have been defined to mimic this behavior. The one that we use here was described in [5, 15]. The algorithm creates the graph by adding one node at the time, and is controlled by two parameters, N and q , where N is the number of node of the final graph and q a parameter that determines connectivity. The graph is built in N steps, indexed by a parameter $t = 1, \dots, N$. At step t , a new node is created, node number t . At this point the graph already has $t-1$ nodes. Let $d(t, i)$, $i = 1, \dots, t-1$ be the number of neighbors of node i at step t . From the newly created node t , q edges are drawn using a *preferential attachment* (or "rich gets richer") strategy: node t is connected to node i with probability

$$P[t \leftrightarrow i] = \frac{d(t, i)}{\sum_{k=1}^{t-1} d(t, k)} \quad (2)$$

The algorithm that generates the graph is shown in Figure 1. The function `prefRnd(V, L)` generates a random element of the set V using the list $L = [d(1), \dots, d(t-1)]$ to determine the probabilities of generating elements of V as in (2). It can be shown that this algorithm generates a power law graph with $P_k \sim k^{-\gamma}$, where the exponent γ depends on the parameter q [15].

```
(V, E) = random_network(n, q)
1.  V ← {1}
2.  E ← ∅
3.  d ← [0|k = 1, ..., n]
4.  for k = 2, ..., n do
5.    V ← V ∪ {k}
6.    for c = 1, ..., q do
7.      u ← prefRnd(d[1], ..., d[k-1])
8.      E ← E ∪ {(k, u)}
9.      d[u] ← d[u] + 1
10.   od
11.   d[k] ← m
12. od
13. return (V, E)
```

Figure 1: The algorithm that generates the preferential attachment graph. The value $d[k]$ keeps track of the number of neighbors of node k at each stage of the construction. The function `prefRnd(V, L)` picks a random element of V with the probabilities given by the elements of L via (2).

```

 $(V, E) = \text{join}(G_y = (V_y, E_y), G_e = (V_e, E_e), \bar{d}_{ey})$ 
1.  $V \leftarrow V_y \cup V_e$ 
2.  $E \leftarrow E_y \cup E_e$ 
3.  $N \leftarrow |V_e| \cdot \bar{d}_{ey}$ 
4.  $d \leftarrow [1|n \in V_y]$ 
5. for  $k \leftarrow 1, \dots, N$  do
6.    $u \leftarrow \text{unif}(V_y)$ 
7.    $v \leftarrow \text{prefRnd}(V_y, d)$ 
8.    $d[v] \leftarrow d[v] + 1$ 
9.    $E \leftarrow E \cup \{(u, v), (v, u)\}$ 
10. od
11. return $(V, E)$ 

```

Figure 2: Algorithm that joins two graphs through preferential attachment. It assumes that $V_y \cap V_e = \emptyset$, that is, the identifiers of the nodes for the elderly and those for the young are different, Both V_y and V_e are ordered list, allowing to maintain the correspondence between the nodes and the values in d . The function $\text{unif}(V)$ returns an element of V chosen randomly with uniform probability.

The complete model is composed of two such graphs interconnected through preferential attachment. First, two power-law graphs are generated. The first is a graph $G_y = (V_y, E_y)$ of young people generated with parameters N_y and q_y ($|V_y| = N_y$), resulting in a graph with exponent γ_y and \bar{d}_y average neighbors per node. The second graph, of elderly people, $G_e = (V_e, E_e)$ is generated with parameter N_e and q_e ($|V_e| = N_e$), resulting in a graph with exponent γ_e and \bar{d}_e average neighbors per node.

Finally, the two graphs are connected: a number \bar{d}_{ey} is selected, which will be the average number of young relations that an elderly person has. Then $N_e \cdot \bar{d}_{ey}$ edges are generated between the two graphs, selecting an elderly person at random with uniform probability, a young person using preferential attachment, and connecting them. The algorithm that joins the two graphs is shown in Figure 2. The rationale for using preferential attachment here is that certain young people (e.g., social workers, cleaning personnel, delivery people, etc.) have contact with many elders, while the majority of young people have little contact with them. The procedure allows us to create a model in which the interrelations within the groups and the relations between groups can be independently controlled.

2.1 Infection dynamics

Each node u of the graph represents an individual which, at any given time t , can be in one of four states, stored in the parameter $\text{state}_t[u]$: *susceptible* (S), *infected* (I), *recovered* (R), or *victim* (V). People transition from one state to another depending on their contacts

$\text{state}_{t-1}[u]$	$\text{state}_t[u]$	with probability
I	R	ϕ
	V	ρ
	I	$1 - \phi - \rho$
R	S	ϵ
	R	$1 - \epsilon$
V	V	1

Table 1: Probabilities of transition for a node from the states I, R, V . Transition from state S to I depends on the contact with the neighbors, and it is not included in this schema (see the text for that transition).

and their recovery probability according to the following diagram:



The only transition that depends on the interaction between nodes is $S \rightarrow I$, whereby a susceptible individual becomes infected. The probability of this transition depends on the parameter β as well as on the number of infected neighbors of a given individual. The model assumes that an individual interacts with their neighbors uniformly³. So, given a node u in state $\text{state}_{t-1}[u] = S$ at time $t - 1$, a node $v \in N(u)$ is picked randomly with uniform probability. If $\text{state}_{t-1}[v] = I$ then, with probability β the node goes to $\text{state}_t[u] = I$ and, with probability $1 - \beta$, it remains in $\text{state}_t[u] = S$.

The other states evolve independently of the state of the neighbors of u , and do so according to the schema of Table 1. These transitions refer to non-vaccinated individuals. A separate indicator for each individual indicates whether the individual was vaccinated. Individuals can be vaccinated only if they are in state S (viz., only healthy individuals are vaccinated), and once vaccinated they will permanently stay in state S (viz., the vaccine is 100% effective).

3 Parameters selection

The model depends on two classes of parameters. On the one hand, *social* parameters ($N_y, N_e, \bar{d}_{ey}; q_y$ and q_e , which determine \bar{d}_y and \bar{d}_e , respectively) determine the structure

³This is the strongest assumption that we make in our model. In reality, of course, each one of us interacts with some of our social relations more often than with others. The problem can be fixed by transforming the graph into a multi-graph, in which the number of edges between two nodes are proportional to the density of contacts between them. We currently have no good model to indicate how these multiple edges should be created.

	\bar{d}_{ey}	
\bar{d}_e	0.5	3.0
1.0	A α	A β
7.7	B α	B β

Table 2: Parameters and codes of the four different graphs we use to analyze the spread of the infection.

of the graph, while *epidemiological* parameters (those of (3) for young and elderly, that is, $\beta_y, \phi_y, \rho_y, \epsilon_y, \beta_e, \phi_e, \rho_e, \epsilon_e$) determine the spread of the infection in each neighborhood of the graph. The epidemic parameters are not observable, but they can be derived based on observable values, as shown in Section 3.2. The observables used here are relative to the early spread of covid-19 in Spain, specifically the period up to March 25, when the effects of the lock-down decreed by the government on March 14 began to have a measurable effect on the spread of the epidemic.

3.1 Social parameters

The tests use graphs with $N = 5,000$ nodes, with 80% of the population being young ($N_y = 4,000$) and 20% being elderly ($N_e = 1,000$). We executed preliminary tests with various values of N , observing that for $N > 1,000$ the results were stable and their qualitative characteristics did not change. The social graph of the young is fixed, generated with $q = 20$, resulting in $\gamma_y = 1.77$ and $\bar{d}_y = 16.9$. These values were chosen to be in compliance with the model in [26]. Then, four different graphs are generated, with different values of the social connection between the elderly (\bar{d}_e) and of the connection between young and elderly (\bar{d}_{ey})⁴. These data result in four graphs, identified by the codes in Figure 2. Graphs of type **A** are characterized by sparse relations between the elderly, that is, each elderly person interacts with few other elderly people, while in graph of type **B** there are many more elderly-to-elderly interactions. Graphs of type α have few cross-age interactions: each elderly person is in contact, on average, with only a few young people, while β graphs have denser interaction. These distinctions will allow us to analyze the effects of different vaccination strategies when used in conjunction with other sanitary measures such as the (relative) isolation of categories at risk or the reduction of contacts between these categories and the general population.

3.2 Epidemiological Parameters

In order to determine the hidden epidemiological parameters ϕ, ρ , and ϵ from observable data, we use an SIR model as a first approximation. At this time, very few cases of reinfection have been reported [3, 12] so, for the time being, one can assume that the immunity is permanent (at least in the time span ϵ considered in the simulation), and set $\epsilon_y = \epsilon_e = 0$.

⁴The actual tests were carried out with 16 graphs with different combinations of these parameters. For the sake of presentation, we show only four graphs, which exemplify the different types of results that we obtained.

Assume a population of $I(t)$ infected people maintained in isolation. In the one-compartment SIR model, their evolution is described by the equations

$$\begin{aligned}\frac{dI}{dt} &= -\phi I - \rho I \\ \frac{dR}{dT} &= \rho I \\ \frac{dV}{dT} &= \phi I\end{aligned}\tag{4}$$

The solution for $I(t)$ is given by

$$I(t) = I_0 \exp(-(\phi + \rho)t)\tag{5}$$

where I_0 is the initial number of infected individuals. The average time a person stays infected before they either die or recover is $1/(\phi + \rho)$. Assuming the day as the time unit, and an average D days duration of the disease, independently of age, one obtains:

$$\phi_y + \rho_y = \phi_e + \rho_e = \frac{1}{D}\tag{6}$$

The values of the individual parameters are determined using the measured lethality, that is, the number of victims divided by the number of cases. Let L_y and L_o be the lethality for young and old people, respectively. From (5) and the first of (4) we have

$$V(t) = \phi \int_0^t I(t) dt = \frac{\phi}{\phi + \rho} I_0 [1 - \exp(-(\phi + \rho)t)]\tag{7}$$

For large t ,

$$V(t) \approx \frac{\phi}{\phi + \rho} I_0\tag{8}$$

Therefore the lethality in terms of the ϕ s and the ρ s can be expressed as

$$\begin{aligned}\frac{\phi_y}{\phi_y + \rho_y} &= L_y \\ \frac{\phi_e}{\phi_e + \rho_e} &= L_e\end{aligned}\tag{9}$$

These equations, together with (4) yield

$$\begin{aligned}\phi_y &= \frac{L_y}{D} \\ \phi_e &= \frac{L_e}{D} \\ \rho_y &= \frac{1}{D}(1 - L_y) \\ \rho_e &= \frac{1}{D}(1 - L_e)\end{aligned}\tag{10}$$

The value of β is derived from its relation to the unitary infection factor R_0 , which is given by

$$R_0 = \frac{\beta}{\phi + \gamma}\tag{11}$$

Observable		Model	
Parameter	Value	Parameter	Value
D	18 days	β_y	0.1333
$R_{0,y}$	2.4	β_e	0.2667
$R_{0,e}$	4.8	ϕ_y	0.0011
L_y	0.02	ϕ_e	0.0111
L_e	0.2	ρ_y	0.0544
		ρ_e	0.044

Table 3: Parameter values used in our simulation. The observable parameters in the first part are derived from the epidemic data for Spain in the period prior to March 30, before the lock-down showed its effects. The unobservable parameters in the second part are derived from those, and are those used in the model.

resulting in

$$\begin{aligned}\beta_y &= \frac{R_{0,y}}{D} \\ \beta_e &= \frac{R_{0,e}}{D}\end{aligned}\tag{12}$$

The values used in the simulations of Section 4 are given in Table 3.

4 Methods

In the first set of simulations, we assume that all vaccination is done on a healthy population before the onset of the epidemic. In the case of an ongoing epidemic such as the one of covid-19, this corresponds to a scenario in which only the still healthy population is considered, keeping it effectively isolated from the people who were already infected. We simulate the different vaccination scenarios given by the parameters specified below and then, once the suitable number of people has been vaccinated, we simulate the unfolding of the epidemic, keeping track of the victims as a function of time. The simulations are characterized by three parameters:

F: Total available vaccine during the period of the simulation, expressed as a fraction of the healthy population that can be vaccinated. We are especially interested in modeling scenarios of scarcity of vaccine. The values used in the simulations are $F = 0.05, 0.1, 0.2$.

ψ : The fraction of the available doses (viz., the fraction of F) that is administered to the elderly. The simulations use the values $\psi = 0, 0.25, 0.5, 0.75, 1$, where $\psi = 0$ means that only the young are vaccinated, while $\psi = 1$ means that only the elderly are vaccinated. The parameters are chosen so that $F \cdot \psi$ is in any case no greater than the fraction of elderly people in the population. If $F \cdot \psi$ is greater than this value then, once all the elderly have been vaccinated, the notion of "vaccination strategy" would cease to be useful: all the vaccine that is left after vaccinating all the elderly would be administered to the young.

mode: The criterion with which the vaccine is administered to the young. The fraction of the vaccine allotted to the elderly is always distributed uniformly inside the group. The fraction that is used to vaccinate the young is allocated according to one of the following modes:

popular: the vaccine is administered in order of "popularity", that is, the nodes in the graphs with the most neighbors are vaccinated first;

connected: the vaccine is administered in order of connections with the elderly: the young people with the most connections to the elderly are vaccinated first.

The rationale for the popular mode is that by vaccinating the people with the most connections will slow down the spread of the infection by removing dangerous "hubs"⁵. The rationale for the connected mode is to protect the vulnerable population by vaccinating the people that can spread the infection from the highly socialized young people (where the spread is rapid) to the less socialized but vulnerable elderly.

The duration of the simulations is fixed and is set to $T = 100$ days.

Mode: **popular**; vaccination level: **5%** ($F = 0.05$)

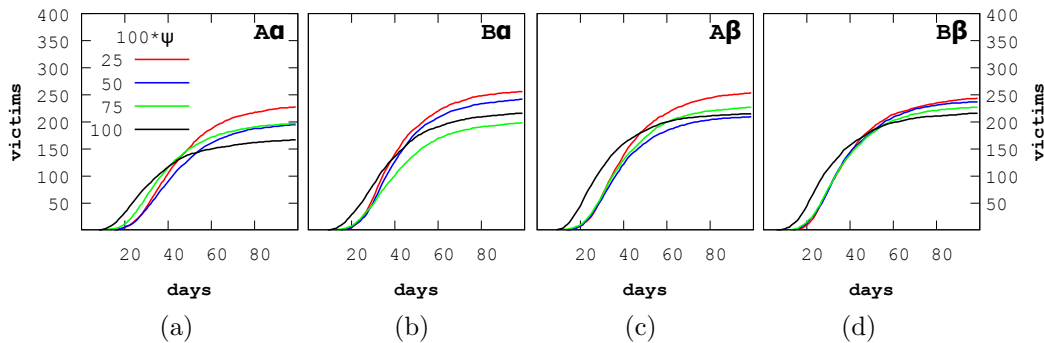


Figure 3: Results for the infinite delivery capacity vaccination. Each curve is drawn for a given fraction of the vaccine administered to the elderly people (0.25, 0.5, 0.75, 1) and tracks the number of victims during the 100 days of the simulation. Here, $F = 0.05$ (5% of the population are vaccinated) and the mode is **popular**.

The second series of simulations assumes a limited capacity to administer the vaccine, so that at most p people can be vaccinated on any given day. The total amount of vaccine available in the given period is still assumed to be sufficient to vaccinate a fraction F of the population (here $F = 0.2$), so the daily vaccination capacity is $p = F/T$ (expressed as the fraction of the population that is vaccinated each day).

In this case the controlled variable is a list $\psi[t]$, $t = 1, \dots, T$, which determines, for each day, the fraction of daily vaccination capacity that is administered to the elderly. That is, on day t , $p \cdot \psi[t]$ elderly people and $p \cdot (1 - \psi[t])$ young people are vaccinated (both these

⁵It is known that the patient zero in parts of Northern Italy was a person that had traveled to China and that, unfortunately, was very popular in his hometown. Meeting with many friends and family in the short time before the onset of symptoms contributed to the rapid initial spread of the virus.

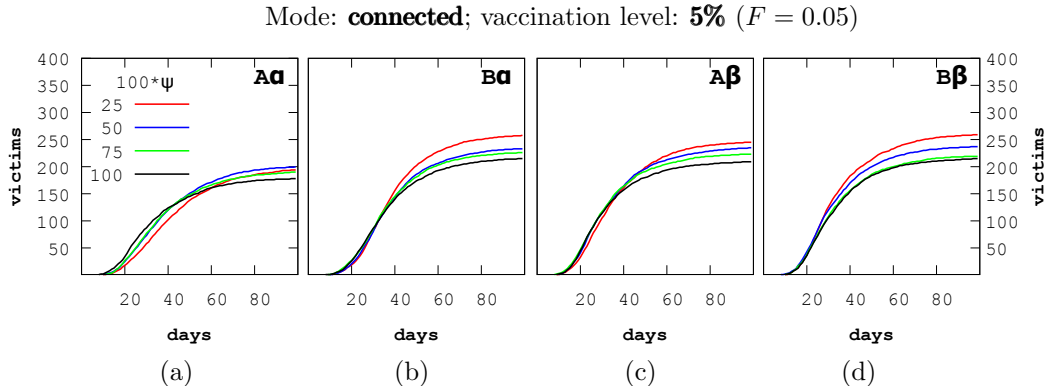


Figure 4: Results for $F = 0.05$ (5% of the population are vaccinated) and mode **connected**. See the caption of Figure 3 for details.

values are expressed as a fraction of the total population). As in the previous case, the elderly to be vaccinated are chosen at random with uniform probability, while the young are chosen according to the selected mode.

For $T = 100$, ψ is a list of 100 values, so it clearly unfeasible and uninformative to sample it and present all the possible sequences in a graph. Instead, we use an optimization algorithm to determine the sequence $\psi[t]$ that minimizes the number of victims during the vaccination period. The optimization is done using a genetic algorithm whose details are given in Appendix A.

5 Results

5.1 One-shot vaccination

In this section, the results are presented in the hypothesis that the delivery capacity is infinite, the only limitation being the amount of vaccine available. The three parameters that affect the results are those in Section 4. On day 0, a number of young and elderly people are vaccinated and from that point on we track the number of fatality for $T = 100$ days. The infection begins at $t = 0$ with one randomly chosen young person infected (the infection never starts with the elderly). Figures 3 and 4 show the data in the hypothesis that the amount of vaccine available is enough to vaccinate 5% of the population. In Figure 3, the young have been vaccinated using the popular mode, while in Figure 4 the connected mode was used.

Each series has four graphs, one for each of the graph types of Table 3, and the four curves in each graph are the victims for different values of ψ , the percentage of doses that are given to the elderly ($\psi = 0.25, 0.5, 0.75, 1$). In almost all cases, at the end of the 100 days, the result is the expected: the number of victims decreases as the fraction of vaccine administered to the elderly increases. The only exception is Figure 4.a, in which the differences are not statistically significant.

The smallest number of victims is achieved in Figure 4.a. This is the graph $A\alpha$, with

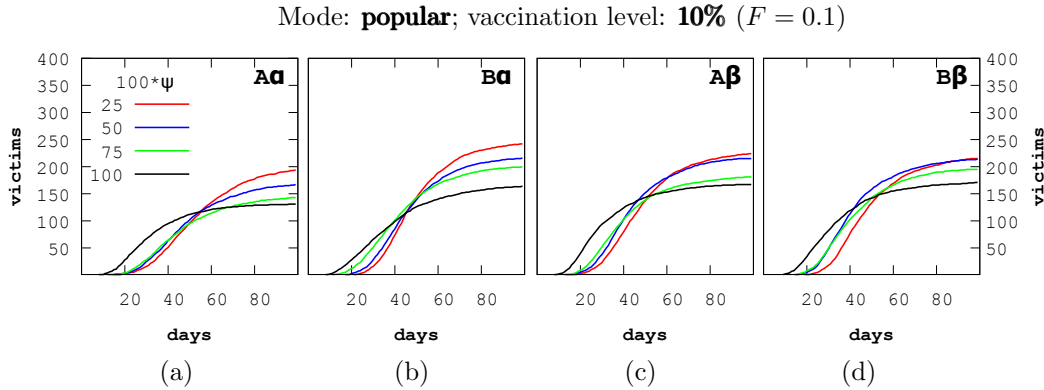


Figure 5: Results for $F = 0.1$ (10% of the population are vaccinated) and mode **popular**. See the caption of Figure 3 for details.

little contact among the elderly and little contact between the elderly and the young. The value is lower in Figure 4.a, the connected mode, suggesting that if the vulnerable population is relatively isolated, vaccinating the (relatively few) contacts is a good strategy.

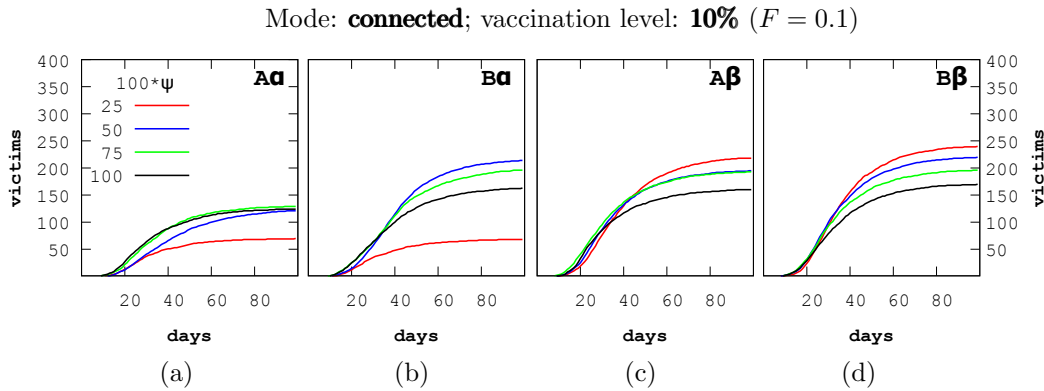


Figure 6: Results for $F = 0.1$ (10% of the population are vaccinated) and mode **connected**. See the caption of Figure 3 for details.

A peculiar phenomenon, which we call *risk inversion* takes place in the popular mode, especially in the $A\beta$ and $B\beta$ graphs: if all doses are given to the elderly ($\psi = 10$) the number of victim in the first 20-30 days is higher than if some of the doses are given to young people. In this case, vaccinating only the elderly does offer some protection to the most vulnerable (albeit an incomplete one: there are, in the case $F = 0.05$, not enough doses to vaccinate all the elderly), but leaves the more heavily connected young completely exposed, leading to a rapid expansion of the epidemic. One the one hand this leads, in the β scenarios in which young and old are more connected, to more victims among the unprotected elderly and, on the other hand, to relatively many victims among the young. On a longer time span, the lack of protection of the elderly for low ψ compensates the effects of slow spreading, and the victims increase when ψ is small.

Mode: **popular**; vaccination level: **20%** ($F = 0.2$)

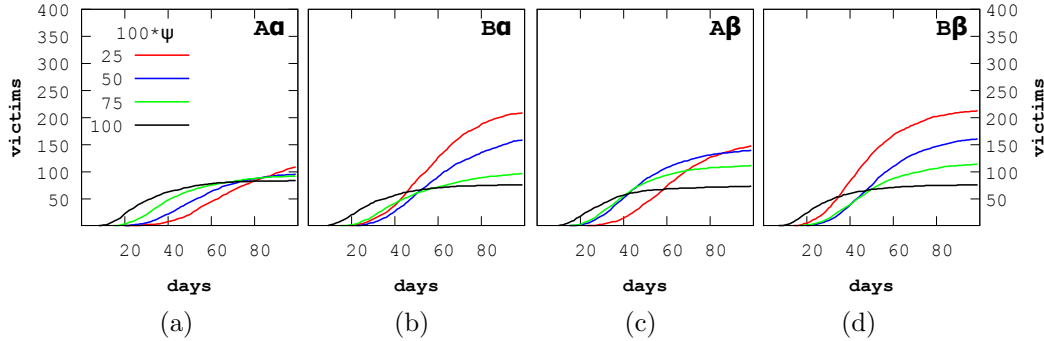


Figure 7: Results for $F = 0.2$ (20% of the population are vaccinated) and mode **popular**. See the caption of Figure 3 for details.

Figures 5 and 6 show the results when 10% of the population is vaccinated, while Figures 7 and 8 are relative to a vaccination level of 20%. Qualitatively, most of the results are similar. It is noteworthy the sharp decrease in mortality in Figure 6.a with respect to Figure 4.a, which suggests that relative social distancing is key to obtain the best results in a situation of scarcity of vaccine. The risk inversion is present here as in the previous cases.

One striking result is that of Figure 6.a and 6.b, in which the mortality behaves opposite as in other cases: giving only 25% of the doses to the elderly results in a significant decrease in mortality. These figures correspond to the *connected* mode of the α graphs, with scarce connection between the elderly and the young. In this situation of high isolation and relatively high availability of doses, using 75% of the vaccine for the connected young effectively isolates the elderly while reducing the victims among the young. Compare this with Figures 8.a and 8.b. In this case, the number of doses is sufficient to provide a better isolation to the vulnerable group, so that in the α graphs the number of victims is low regardless the value of ψ . In the β graph of Figure 8.b, the stronger connection between elderly and young balances out the higher number of doses available, and the phenomenon of Figure 6.a is repeated. The convenience of targeting the "connection points" (the young people that have connections with the vulnerable population) depends on the amount of vaccine available and on the density of the relations between elderly and young.

The risk inversion in the early days of vaccination is present in all cases, although not with the same prominence. This phenomenon suggests that if the vaccine is available in batches, the vaccination policy might be different for different batches: a first vaccination in part to the young to limit the speed of the infection and, if a second batch is available within 20 or 30 days, a more massive vaccination to the elderly to protect them.

5.2 Incremental vaccination

Figures 9 and 10 show the optimal vaccination schedule as determined by the optimization algorithm. The vaccination schedule is assumed to extend over a period of 100 days, and the total number of doses is assumed to be sufficient to vaccinate 20% of the population.

Mode: **connected**; vaccination level: **20%** ($F = 0.2$)

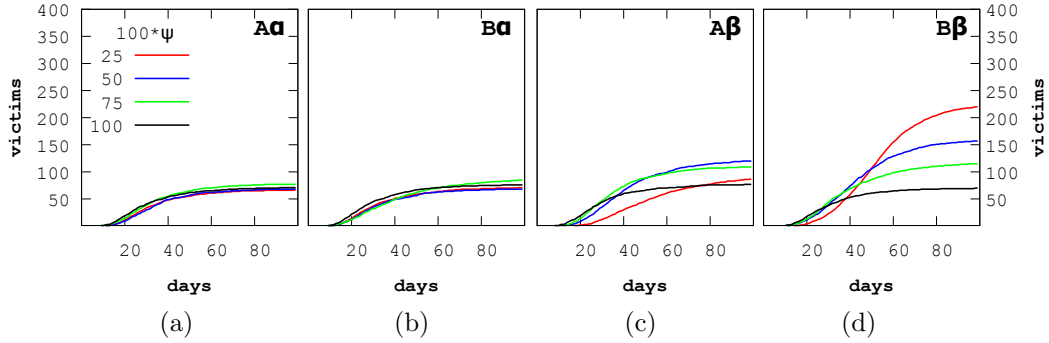


Figure 8: Results for $F = 0.2$ (20% of the population are vaccinated) and mode **connected**. See the caption of Figure 3 for details.

The results were obtained using 500 generations of 800 genes each (see Appendix A). The results of the best genes of several generations were checked to verify that the solutions were stable. In the figures, the black crosses mark the output of the optimizer, that is, they represent the optimal fraction of vaccine to be administered to the elderly each day. The red line is a polynomial least squares approximation of these data using a polynomial of degree 10, which allows us to detect the general trends of the solution without the abrupt changes: our considerations will be based on these curves. The blue and green lines are the victims among the young and old people respectively, expressed as a fraction of the respective population. In Figure 9 the vaccination of the young is done using the popular mode, while in Figure 10 the connected mode was used. The four graphs in each figure are relative to the four graph types of Table 3.

Mode: **popular**

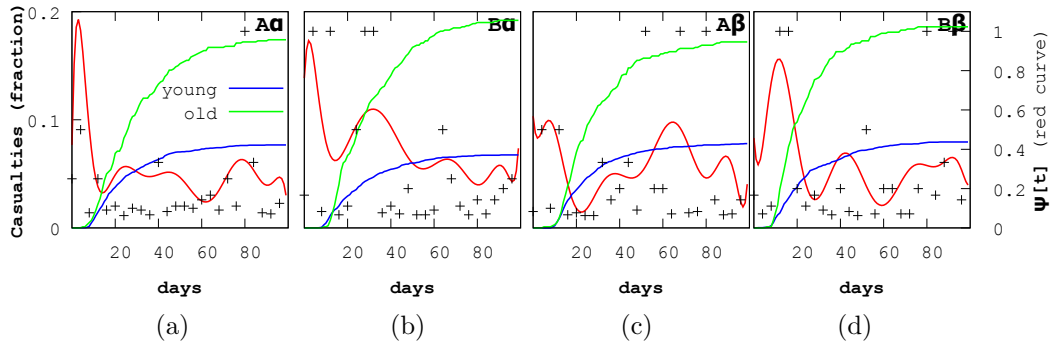


Figure 9: Optimal vaccination strategy and the resulting mortality. The black crosses are the output of the optimizer; the red line is a polynomial approximation (degree=10) that highlights the general trends of the solution, the blue and green lines are the fraction of the young and elderly that have died, respectively, each one expressed as a fraction of the respective population. The vaccination of the young is done using the popular mode: the young people most connected are vaccinated first.

One common feature of all the strategies is the high initial fraction of vaccine administered to the elderly followed by an increase in vaccine given to the young when the number of casualties begins to grow. The peaks are more pronounced in the popular mode: in this case, after an initial short vaccination period to protect part of the vulnerable population, the focus moves to the young in order to stop the spread of infection by cutting the social hubs through vaccination. The situation is less clear in the β graphs (with many connections between the two groups). In this case, especially in the $A\beta$ graph, the optimal strategy seems to involve a more balanced approach, with alternating focus on the elderly and the young.

For the connected mode, in the α graphs, the peak of vaccination of the elderly is wider. Given the low value of \bar{d}_{ey} , relatively few vaccinations of the young are sufficient to block the spread of the infection to the vulnerable population, so the initial vaccination effort can concentrate on the vulnerable for a longer period of time. In the $A\beta$ graph, with few elderly-to-elderly relations and strong connections with the young, the focus shifts on a much earlier vaccination of the young.

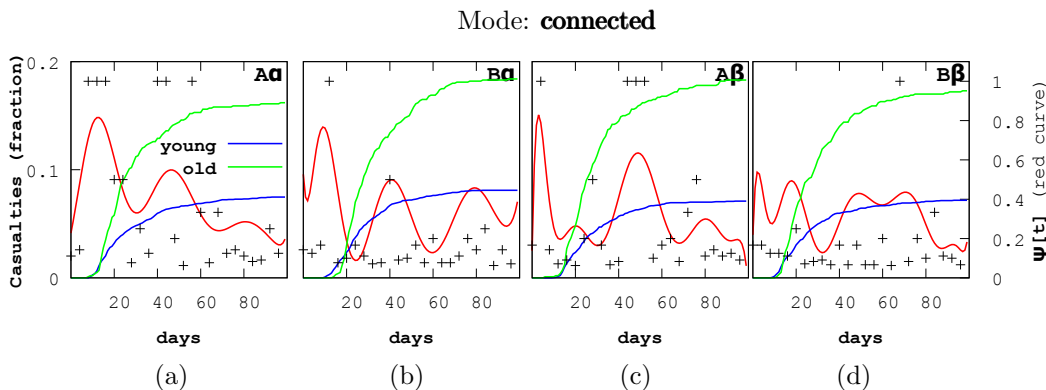


Figure 10: Optimal vaccination strategy and the resulting mortality. The black crosses are the output of the optimizer; the red line is a polynomial approximation (degree=10) that highlights the general trends of the solution, the blue and green lines are the fraction of the young and elderly that have died, respectively, each one expressed as a fraction of the respective population. The vaccination of the young is done using the connected mode: the young people most connected to the elderly are vaccinated first.

6 Conclusions

We have developed a model that, with respect to the standard SIR model, allows us to take into account the variability of the social relations of people in a social scenario. Given the existence of social groups especially vulnerable to the disease (herein referred to as "the elderly"), two factors appear crucial when defining a vaccination strategy: the social relations among the elderly, and the connections between the elderly and the young.

The most general result that we can draw from the model is that a prudent vaccination

strategy should balance two requirements: protect the elderly, and vaccinate enough young people (with intense social relations) to slow down the spread of the infection.

The exact nature of this balance depends on the social connections and on who, among the young people, is vaccinated. Overall, the most effective strategy seems to be to give priority, among the young, to those who are more heavily connected to the vulnerable people (caregivers, cleaning personnel, etc.). If the amount of available vaccine is not too scarce (at least 10% of the population in our simulations), the results are good even if only 25% of the doses is administered to the vulnerable. If additional measures are taken to keep the vulnerable isolated, the 25% solution is actually the one that gives the best results. If the elderly are not isolated, then the strategy of splitting the vaccine between them and the young has positive results in a short (20-30 days) period but, in a longer period, it is necessary to move to a heavier vaccination to the vulnerable.

A more detailed strategy can be devised if we take into account a limited delivery capacity and the distribution of the vaccination over the whole duration of the epidemic. In this case, the optimal strategy seems to begin with a higher fraction of elderly vaccinated then, when the number of victims begins to grow, with a more intense vaccination of young people to keep the spread under control. The strategy that follows this first phase is less clear, but it appear to always consist in an oscillation with periods of more intense vaccination of the elderly alternated with periods of more intense vaccination of the young, all with a general tendency to increase the fraction of vaccine administered to the young.

A few words of caution are in order. All these results were obtained through a mathematical model in which, necessarily, many of the details of the actual situation are abstracted. While the general conclusions that we derived have undoubtedly a validity, applying them in the field requires extreme caution and a deeper analysis of the evolution of the epidemic.

Also, our model has assumed that the "most popular" and "most connected" people can be identified and summoned for vaccination. This hypothesis might be reasonably realistic for the connected mode, in which the focus can often be identified by profession than with the more elusive popular mode. The distribution of the number of neighbors of the node one arrives to when crossing a random edge [21] may help implementing this mode.

Finally, we have ignored here all the problems of public perception, and the media backlash that may be caused by a strategy that, rational as it might be, does not follow what the people (or, more importantly, the media) perceive as "common sense".

References

- [1] Daron Acemoglu, Victor Chernozhukov, Iván Werning, and Michael D Whinston. Optimal targeted lockdowns in a multi-group sir model. *NBER Working Paper*, 27102, 2020.
- [2] Syed Faraz Ahmed, Ahmed A Quadeer, and Matthew R McKay. Preliminary identification of potential vaccine targets for the covid-19 coronavirus (sars-cov-2) based on sars-cov immunological studies. *Viruses*, 12(3):254, 2020.

- [3] Javad Alizargar. Risk of reactivation or reinfection of novel coronavirus (covid-19). *Journal of the Formosan Medical Association*, 2020.
- [4] Alex Arenas, Leon Danon, Albert Diaz-Guilera, Pablo M Gleiser, and Roger Guimera. Community analysis in social networks. *The European Physical Journal B*, 38(2):373–80, 2004.
- [5] Albert-László Barabási and Réka Albert. Emergence of scaling in random networks. *science*, 286(5439):509–512, 1999.
- [6] Andrew Barbour and Denis Mollison. Epidemics and random graphs. In *Stochastic processes in epidemic theory*, pages 86–9. Springer, 1990.
- [7] Tom Britton, Svante Janson, and Anders Martin-Löf. Graphs with specified degree distributions, simple epidemics, and local vaccination strategies. *Advances in Applied Probability*, 39(4):922–48, 2007.
- [8] Luis E Escobar, Alvaro Molina-Cruz, and Carolina Barillas-Mury. Bcg vaccine protection from severe coronavirus disease 2019 (covid-19). *Proceedings of the National Academy of Sciences*, 117(30):17720–6, 2020.
- [9] Marta C Gonzalez, Cesar A Hidalgo, and Albert-Laszlo Barabasi. Understanding individual human mobility patterns. *Nature*, 453(7196):779–782, 2008.
- [10] Herbert W Hethcote. The mathematics of infectious diseases. *SIAM review*, 42(4):599–653, 2000.
- [11] Mangalakumari Jeyanathan, Sam Afkhami, Fiona Smaill, Matthew S Miller, Brian D Lichty, and Zhou Xing. Immunological considerations for covid-19 vaccine strategies. *Nature Reviews Immunology*, pages 1–18, 2020.
- [12] Robert D Kirkcaldy, Brian A King, and John T Brooks. Covid-19 and postinfection immunity: Limited evidence, many remaining questions. *Jama*, 323(22):2245–6, 2020.
- [13] Archana Koirala, Ye Jin Joo, Ameneh Khatami, Clayton Chiu, and Philip N Britton. Vaccines for covid-19: The current state of play. *Paediatric respiratory reviews*, 35:43–9, 2020.
- [14] David Lazer, Alex Pentland, Lada Adamic, Sinan Aral, Albert-Laszlo Barabasi, Devon Brewer, Nicholas Christakis, Noshir Contractor, James Fowler, Myron Gutmann, et al. Social science. computational social science. *Science (New York, NY)*, 323(5915):721–3, 2009.
- [15] Jure Leskovec, Lars Backstrom, Ravi Kumar, and Andrew Tomkins. Microscopic evolution of social networks. In *Proceedings of the 14th ACM SIGKDD International Conference on Knowledge Discovery and Data Mining*, pages 462–70. ACM, 2008.
- [16] Nicole Lurie, Melanie Saville, Richard Hatchett, and Jane Halton. Developing covid-19 vaccines at pandemic speed. *New England Journal of Medicine*, 382(21):1969–73, 2020.

- [17] Melanie Mitchell. *An introduction to genetic algorithms*. Cambridge, MA:MIT press, 1998.
- [18] Lev Muchnik, Sen Pei, Lucas C Parra, Saulo DS Reis, José S Andrade Jr, Shlomo Havlin, and Hernán A Makse. Origins of power-law degree distribution in the heterogeneity of human activity in social networks. *Scientific reports*, 3(1):1–8, 2013.
- [19] Mark J Mulligan, Kirsten E Lyke, Nicholas Kitchin, Judith Absalon, Alejandra Gurtman, Stephen Lockhart, Kathleen Neuzil, Vanessa Raabe, Ruth Bailey, Kena A Swanson, et al. Phase 1/2 study of covid-19 rna vaccine bnt162b1 in adults. *Nature*, pages 1–5, 2020.
- [20] Mark EJ Newman, Steven H Strogatz, and Duncan J Watts. Random graphs with arbitrary degree distributions and their applications. *Physical review E*, 64(2), 2001.
- [21] M.E.J. Newman. Threshold effects for two pathogens spreading on a network. *Physical Review Letters*, 95(108701), 2005.
- [22] Gergely Palla, Albert-László Barabási, and Tamás Vicsek. Quantifying social group evolution. *Nature*, 446(7136):664–7, 2007.
- [23] Junkichi Satsuma, R Willox, A Ramani, B Grammaticos, and AS Carstea. Extending the sir epidemic model. *Physica A: Statistical Mechanics and its Applications*, 336(3-4):369–75, 2004.
- [24] Matthew D Shin, Sourabh Shukla, Young Hun Chung, Veronique Beiss, Soo Khim Chan, Oscar A Ortega-Rivera, David M Wirth, Angela Chen, Markus Sack, Jonathan K Pokorski, et al. Covid-19 vaccine development and a potential nanomaterial path forward. *Nature Nanotechnology*, 15(8):646–55, 2020.
- [25] Boris Shulgin, Lewi Stone, and Zvia Agur. Pulse vaccination strategy in the sir epidemic model. *Bulletin of mathematical biology*, 60(6):1123–48, 1998.
- [26] Ignacio Tamarit, José A Cuesta, Robin IM Dunbar, and Angel Sánchez. Cognitive resource allocation determines the organization of personal networks. *Proceedings of the National Academy of Sciences*, 115(33):8316–21, 2018.
- [27] Dashun Wang, Dino Pedreschi, Chaoming Song, Fosca Giannotti, and Albert-Laszlo Barabasi. Human mobility, social ties, and link prediction. In *Proceedings of the 17th ACM SIGKDD international conference on Knowledge discovery and data mining*, pages 1100–8, 2011.

A Optimization of the vaccination schedule

Mathematically, our problem is the following. We have a multidimensional variable, the values $\psi[t] \in [0, 1]$, $t = 1, \dots, T$ ($T = 100$ in our case), and a function $G(\psi)$ that we want to minimize. In this case, $G(\psi)$ is the number of fatalities for the infection when ψ is

used as a vaccination schedule (fraction of the vaccination that is given to the elderly each day). The value of G is not a trivial function of ψ . In particular, we cannot assume any of the standard properties (continuity, derivability, analiticity, etc.) that most optimization algorithms assume. Because of the nature of the function, a genetic algorithm [17] is a reasonable option to solve this optimization problem.

We transform the problem into a discrete one by restricting $\psi[t]$ to values of the type

$$\psi[t] = \frac{1}{n[t] + 1} \tag{13}$$

with $n[t] \in [0, 15]$. Each $n[t]$ can be represented as a four-bit number, so the sequence $n[1], \dots, n[T]$ that determines the solution can be represented as an integer of $4 \cdot T$ bits. This is the "gene" of our algorithm.

A generation is composed of a collection of G genes γ_i , $i = 1, \dots, G$. Given a gene, we derive from it the vaccination schedule using (13) and execute the simulation. This will result in a score s_i . Standard genetic algorithms are function maximizers, so we consider as score the inverse of the number of fatalities at time T ($s_i = -V_{\gamma_i}(T)$). There are several

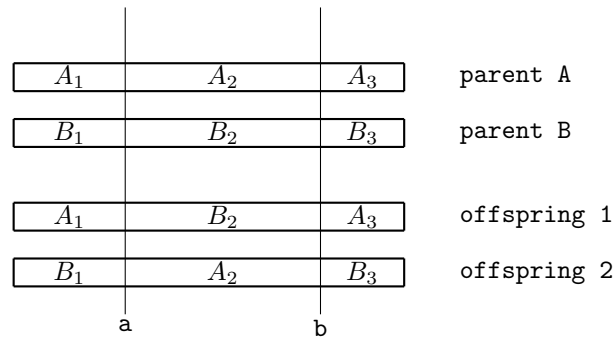


Figure 11: Double cut for the generation of offspring. Two parents generate two offspring, mixing the bits of their genes as represented.

methods to create the following generation of individuals. Since the performance of the algorithms seems to have little dependence in the specific method used, we use one of the simplest, based on the creation of an intermediate *gene pool*. The gene pool is a set \mathcal{P} of P individuals possibly replicated (generally $|P| = G$: the pool has the same size as the generations) such that the number of "copies" of an individual in the pool is proportional to its score. An easy algorithm for generating a pool is the *tournament*: we do P comparisons of pairs of individuals taken at random from the generation: the individual with the highest score goes into the pool:

```

P ← ∅
for k=1 to P do
  i ← rnd(1,G)
  j ← rnd(1,G)
  if si ≥ sj then
    P ← P ∪ {γi}
  else
    P ← P ∪ {γj}
fi
od

```

In order to build the next generation, pairs of genes are taken at random from the pool (with uniform distribution) and crossed to create two new individuals that will go into the next generation (this requires that G be even). We use the method of the *double cut* to cross the genes. Two values $a, b \in [0, 4T]$ are chosen randomly. The two offspring are then generated as in Figure 11, in which we assume $a < b$. We also define a small mutation probability: for each new gene, with a (small) probability p , we pick a random bit and flip it. Note that this method doesn't guarantee that the best individual of a generation will pass unchanged to the next, so we actually use the crossing to create $G - 2$ individuals to which we add the two best performers of the previous generation.